

Demystifying Transmission Lines: What are they, Why are they useful?

Introduction:

Porous electrodes offer a high surface area to volume or weight ratio which is highly beneficial to a number of energy generation or storage devices. (e.g. Dye-Sensitized Solar Cells, Super-Capacitors, Fuel Cells, etc). Transmission lines are heavily used in modeling in Electrochemical Impedance Spectroscopy (EIS) experiments where porous systems are employed.

Though transmission lines are commonly used, an introductory paper was hard to find. This paper is intended to serve that purpose. It assumes basic knowledge of EIS and modeling using equivalent circuits as covered in our EIS application note.

Nomenclature and Notation:

We will distinguish between the base electrode and the porous electrode and the various interfaces as shown in Figure 1.

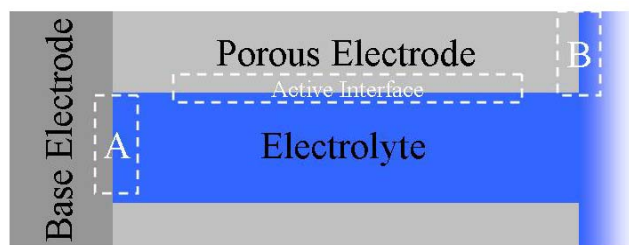


Figure 1 Porous electrodes and the nomenclature that will be used in this paper.

There are three regions that are of interest to the electrochemist. These are marked A, B, and Active Interface in Figure 1. A and B represent the interfaces between the base

electrode and tip of the porous electrode with the electrolyte solution respectively. The active interface is the interface between the porous electrode and the electrolyte and this is the interface in question in most of the transmission line applications.

The base electrode and the porous electrode are electrically connected and generally based on the same material. For most systems, however, they behave sufficiently differently at the interface with the electrolyte that maintaining this distinction is useful.

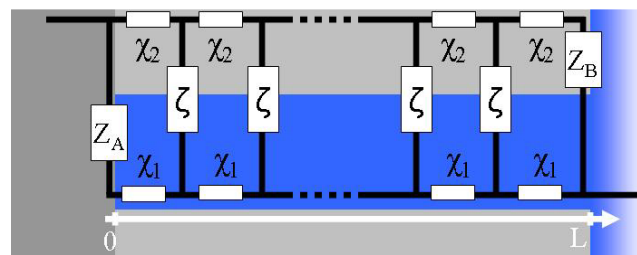


Figure 2 Transmission Line. χ_1, χ_2, ζ are the repeating circuit blocks on the rails and the steps. Z_A and Z_B correspond to impedances across the interfaces A and B defined in Figure 1.

A transmission line model in generic form is shown in Figure 2. $\zeta, \chi_1, \chi_2, Z_A$ and Z_B are defined as subcomponents that can take various forms. These may be as basic as single resistors and as complicated as necessary. χ_1, χ_2 , and ζ represent the solution impedance, bulk the impedance of the porous electrode material, and the impedance of the active interface respectively. We will refer to

χ_1 and χ_2 as rail impedances and ζ as the step impedance using a ladder analogy. Z_A and Z_B are the impedances of the two interfaces A and B shown in Figure 1.

The parameter L represents the length of the transmission line (or the depth of the pore) as shown in Figure 2. It can be visualized as the number of steps in the ladder. Once the fitting is done, the numbers that are characteristic of the sample are $\chi_1 L$, $\chi_2 L$ and ζ/L . The value and the units of L has to be decided on before the fitting is attempted and has to be locked to a particular value. We will assume L to be unitless for this paper to keep this discussion straightforward. In practice, knowledge of the thickness L allows to determine important parameters such as the conductivity and diffusion coefficient from the impedance fit results.

When defining the subcomponents, we will use capital letters for components that do not repeat and lowercase letters for components that do. We will represent resistors with an R (or r) and constant phase elements with a Q (or q). The symbol “|” will be used to indicate a parallel combination of the components.

The generic equation governing the impedance of the entire line shown in Figure 2 is (from Bisquet, J.¹):

$$Z = \frac{1}{\chi_1 + \chi_2} \left[\frac{\lambda(\chi_1 + \chi_2)S_\lambda + (Z_A + Z_B)C_\lambda}{\frac{Z_A Z_B S_\lambda}{\lambda(\chi_1 + \chi_2)}} \right]^{-1} \times \left\{ \begin{array}{l} L\lambda\chi_1\chi_2(\chi_1 + \chi_2)S_\lambda + \chi_1[\lambda\chi_1 S_\lambda + L\chi_2 C_\lambda]Z_A \\ + \chi_2[\lambda\chi_2 S_\lambda + L\chi_1 C_\lambda]Z_B \\ + \left[2\chi_1\chi_2 + (\chi_1^2 + \chi_2^2)C_\lambda + \frac{L}{\lambda}\chi_1\chi_2 S_\lambda \right] \frac{Z_A Z_B}{\chi_1 + \chi_2} \end{array} \right\} \quad (1)$$

Where $C_\lambda = \cosh(L/\lambda)$, $S_\lambda = \sinh(L/\lambda)$ and $\lambda = [\zeta/(\chi_1 + \chi_2)]^{1/2}$.

In the Echem Analyst:

In the Echem Analyst, the circuit in Figure 3 is implemented with $\chi_1 \equiv r_1$, $\zeta \equiv r_3 || q_3$, $\chi_2 \equiv r_2$, $Z_A \equiv R_A || Q_A$ and $Z_B \equiv R_B$ as shown in Figure 3 and named “Unified”. These blocks were implemented using the procedure described in our “User Defined Components” application note. They can easily be modified for specific needs and incorporated into the model. Detailed instructions can be found in our Technical Note regarding the implementation of Transmission Lines.

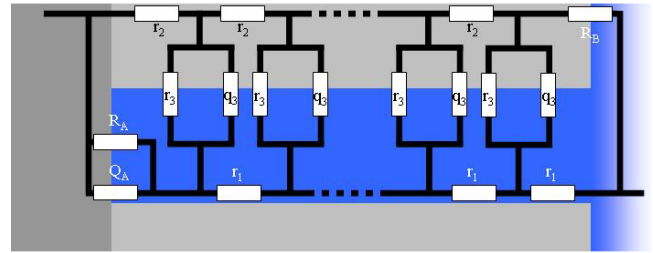


Figure 3 The specific model implemented in Echem Analyst as “Unified” where $\chi_1 \equiv r_1$, $\zeta \equiv r_3 || q_3$, $\chi_2 \equiv r_2$, $Z_A \equiv R_A || Q_A$ and $Z_B \equiv R_B$

Limiting cases can be easily achieved by adjusting the appropriate elements to be zero or very large. However, two models shown in Figure 4 are very commonly employed in the literature and are worthy of specific mention. Originally developed by Bisquet, J.ⁱⁱ to model diffusion- recombination processes, they have been applied to dye-sensitized solar-cellsⁱⁱⁱ, supercapacitors and a number of other areas.

We will follow the notation assumed by Bisquet, J.ⁱⁱ and use $\chi_1 \equiv 0$, $\zeta \equiv \zeta_m$, $\chi_2 \equiv \chi_m$, $Z_A \equiv \infty$ and $Z_B \equiv \infty$ (Figure 4a) or $Z_B \equiv 0$ (Figure 4b). The impedance equations are:

$$Z = \sqrt{\zeta_m \cdot \chi_m} \coth \left(L \cdot \sqrt{\frac{\chi_m}{\zeta_m}} \right) \quad \text{(Figure 4a)} \quad (3)$$

$$Z = \sqrt{\zeta_m \cdot \chi_m} \tanh \left(L \cdot \sqrt{\frac{\chi_m}{\zeta_m}} \right) \quad \text{(Figure 4b)}$$

In the Echem Analyst, these models are named “Bisquet Open (BTO)” (Eq. 3a) and “Bisquet Short (BTS)” (Eq. 3b) with $\chi_m \equiv r_m$, $\zeta_m \equiv r_k || q_k$.

These models are very useful since it is typical to find in applications where the conductivity of one rail is much larger than the other one. These cases can be modeled well with one rail set to zero.

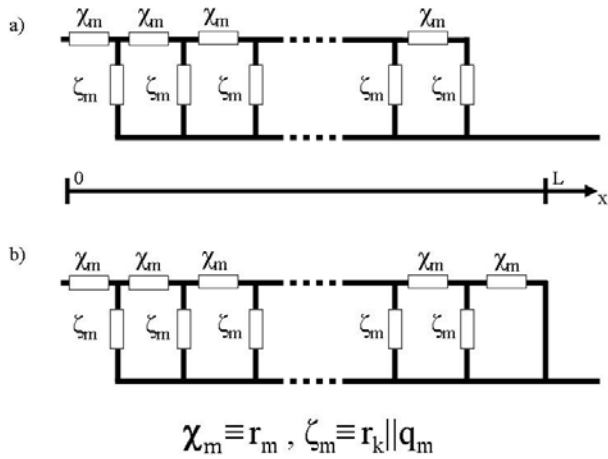


Figure 4 Two specific cases where χ_2 is shorted, Z_A is open circuit and Z_B is either open circuit or short circuit, from Bisquert *et. al.*ⁱⁱ These are defined as Bisquert Open (BTO) (a) and Bisquert Short (BTS) (b) in the Echem Analyst.

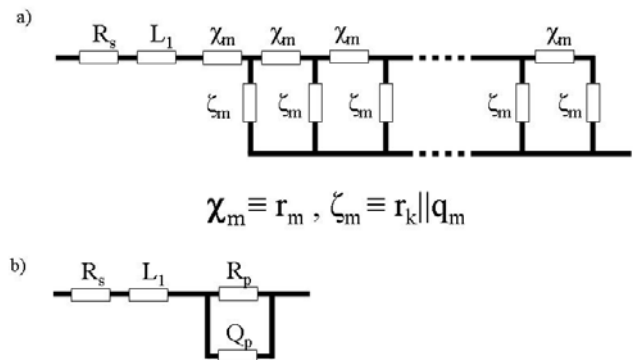


Figure 5 Two models that are used to fit the capacitor data in figure 6. a) The transmission line model, b) R-CPE model.

Applications:

UltraCapacitors:

Ultracapacitors are currently being developed to generate strong energy bursts for a number of applications including uninterruptible power supplies, lasers, and power electronics for electric and hybrid vehicles. They provide a very high capacitance in a relatively small volume and weight utilizing porous materials that have very high specific surface areas.

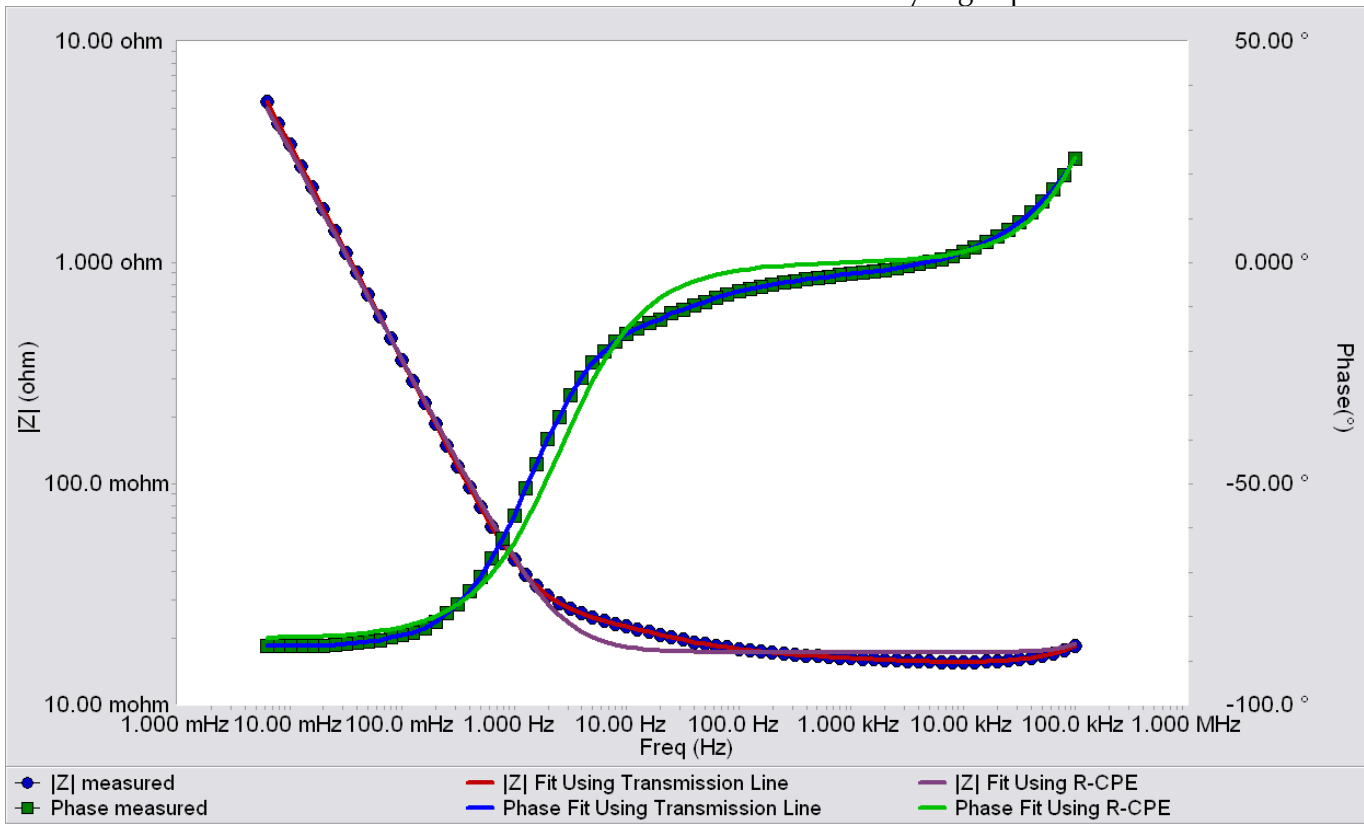


Figure 6 EIS data of an ultracapacitor and the fits using a transmission line and a resistor and a constant phase element in parallel. The circuit models used are shown in Figure 6 and the fit results are shown in table1

Figure 6 shows the impedance spectra and the fits of a 5F capacitor¹ at 0V DC and 1mV (rms) AC.

To fit the data we have tried the models shown in Figure 5. As seen in figure 6 the fit is excellent over the entire frequency range when the transmission line model is used and poor when R-CPE model is used. During the fit using the “Bisquert Open” model, parameter L was locked to 0.001 and R_k was locked to $10^{35}\Omega$. These values have a gray background in table1. As the fit shows the R-CPE model misses a feature in the frequency range 10Hz-100Hz. The Y_o value that comes out of the fit (after the L scaling described in the introduction) is $4.346 S s^{-0.975}$ (notice $S s^1$ would be F).

R_s	0.0156	ohms
L	0.001	
r_m	22.06	ohm
r_k	10^{35}	ohm
y_m	4346.00	$S s^a$
a	0.975	
L_1	12.50	nH

Table 1 Fit results for 5F capacitor using the model shown in Figure 6a. L and R_k were locked during the fit. R_k was chosen to simulate an open circuit.

Dye-Sensitized Solar Cells

Dye-Sensitized solar cells (DSC) are another application where transmission line models are regularly employed. Briefly, these are solar cells that utilize an organic or an organometallic dye molecule adsorbed on mesoporous TiO_2 to absorb sunlight efficiently. The excited electrons are then extracted out through the TiO_2 . Again, the use of a porous electrode warrants the use of transmission lines.

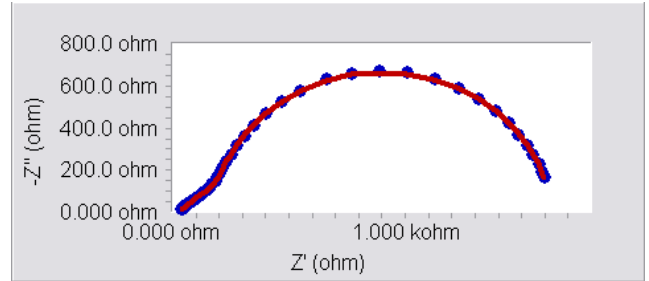


Figure 7 The DSC data and the fit using "Bisquert Open"

Figure 7 shows an impedance spectra of a DSC made using porous TiO_2 . The spectrum is fit using a “Bisquert Open” model and the fit is excellent over the entire frequency range. The fit results are summarized in table 2

R_s	26.27	ohm
L	1.00	
r_m	469.20	ohm
r_k	1452.00	ohm
y_m	1.84E-04	$S s^a$
a	0.94	

Table 2 Fit results for DSC impedance spectra shown in Figure7 fit using a “Bisquert Open” and a resistor in series.

In certain types of DSCs where an organic hole conductor is used instead of a liquid electrolyte the region A is not insulating. The circuit model has to include a parallel resistance and constant phase element combination to account for region A as shown in figure 7. This type of model is employed in the literature to model this and other types of DSCs^{iv}.

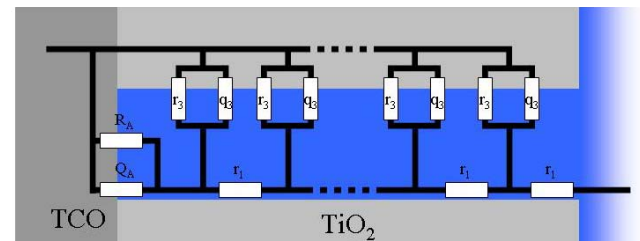


Figure 7 Circuit model describing a TiO_2 /Organic Conductor DSC. (TCO = Transparent Conducting Oxide)

¹ ESHSR-0005C0-002R7 from Ness Capacitor , Gyeonggi-do, Korea

Q_A and q_3 denote the constant phase elements between the base electrode / electrolyte and the porous electrode / electrolyte, respectively. Notice χ_1 is assumed to be short circuit and Z_B is assumed to be open circuit. The data for this case is depicted in Figure 8.

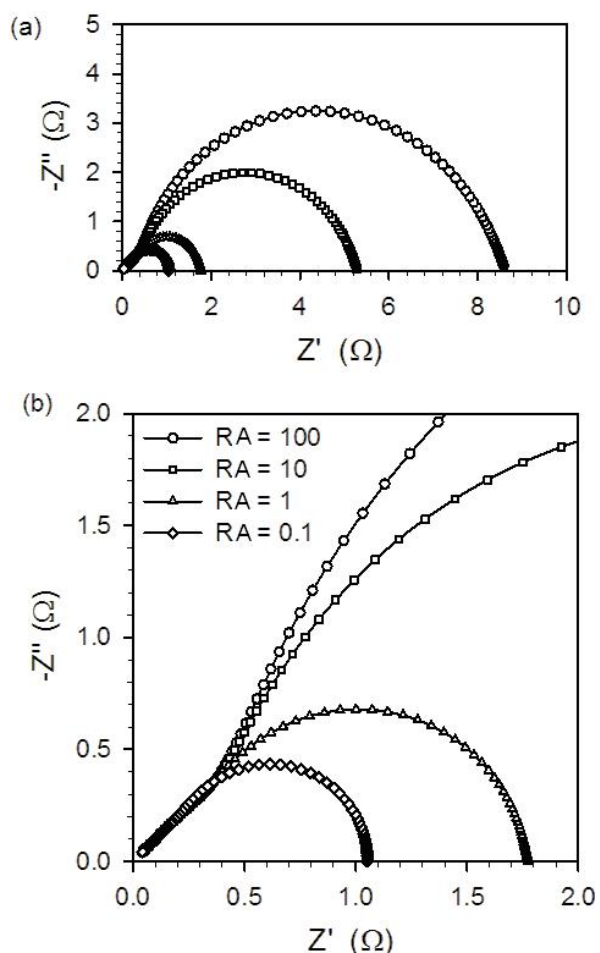


Figure 8 The simulated data for the circuit depicted in Figure 5 for $r_1= 10^6 \Omega$, $r_3=9.10^{-6} \Omega$, $q_3=5.10^3$, $a_3=1$, $Q_A=10^{-2}$, $a_A=0.7$, and R_A takes four different values shown in the legend.

Though it is possible to generate the mathematical expressions for this and other particular cases (and it is done in the literature, see for example Bisquert, J. ¹), one can also use “Unified”(Figure 3) to fit this and other cases by adjusting the appropriate parameters to be zero or very large.

In order to employ Unified in fitting the data shown in figure 8 we need to force r_2 to be a short circuit (i.e. $r_2=0 \Omega$) and R_B to be an open circuit (i.e. $R_B \rightarrow \infty$ or numerically R_B should be much larger than any other relevant resistance in the fitting or the data). These values were locked during the fitting, and have a gray background in table 2.

	RA=0.1	RA=1	RA=10	RA=100
L	10^{-6}	10^{-6}	10^{-6}	10^{-6}
r₁	10^6	10^6	10^6	10^6
r₂	0	0	0	0
r₃	9.19×10^{-6}	9.07×10^{-6}	9.07×10^{-6}	9.00×10^{-6}
Y_{o3}	5.01×10^3	5.00×10^3	5.02×10^3	5.00×10^3
a₃	1	1	1	1
Y_{oA}	9.42×10^{-3}	0.01	0.01	0.01
R_A	0.0978	0.998	9.897	100.1
a_A	0.717	0.700	0.699	0.700
R_B	10^{35}	10^{35}	10^{35}	10^{35}

Table 3 The fit parameters for the Unified model and the four data sets shown in Figure 6. The gray rows indicate the parameters that were locked during the fit. Notice r_2 was locked to be a short circuit and R_B was locked to open circuit. The top row corresponds to the legend of figure 8.

Conclusion:

Porous electrodes are regularly utilized for applications where a high surface area is beneficial. Impedance spectroscopy on porous materials regularly results in data that cannot be modeled with standard circuit components. Transmission lines are required due to the distributed nature of the interfacial impedance throughout the pore.

Acknowledgements:

We gratefully acknowledge the data and very useful comments from Prof. Juan Bisquert and Dr. Francisco Fabregat-Santiago in the process of writing this paper.



C3 PROZESS- UND
ANALYSENTECHNIK GmbH
Peter-Henlein-Str. 20
D-85540 Haar b. München
Telefon 089/45 60 06 70
Telefax 089/45 60 06 80
info@c3-analysentechnik.de
www.c3-analysentechnik.de

734 Louis Drive • Warminster PA 18974 • Tel. 215 682 9330 Fax 215 682 9331 • www.gamry.com • info@gamry.com

ⁱ Bisquert, J. *Phys. Chem. Chem. Phys.*, 2000,**2**, 4185-4192

ⁱⁱ Bisquert, J. *J. Phys. Chem. B* 2002, **106**, 325-333

ⁱⁱⁱ Wang, Q.; Moser, J.-E.; Grätzel, M. *J. Phys. Chem. B* 2005, **109**, 14945-19453

^{iv} Fabregat-Santiago, F.; Bisquert, J.; Garcia-Belmonte, G.; Boschloo, G.; Hagfeldt, A. *Sol. Ener. Mat. & Sol. Cells* 2005, **87**, 117-131